ELECTRICAL PROPERTIES OF DC REACTIVE MAGNETRON SPUTTERED ZnO:Al FILMS FROM OPTICAL SPECTRA

PD Nsimama[1] and ME Samiji[2]
[1]Department of Science and Laboratory Technology, Dar Es Salaam Institute of Technology, P.O. Box 2958, Dar Es Salaam, Tanzania
[2]Physics Department, University of Dar Es Salaam, Tanzania, P.O. Box 35063, Dar Es Salaam, Tanzania
Correspondence: pnsimama@yahoo.com, nsimama@dit.ac.tz

ABSTRACT
Reactive direct current (DC) sputtered ZnO:Al films were prepared using the plasma emission monitoring (PEM) system. Films were deposited using PEM setpoints ranging from 50 to 80%. Transmittance and reflectance of the films were measured by using the UV-VIS-NIR Lambda 900 double beam spectrophotometer. The sheet resistance was measured using the four-point probe. Films optical spectra were fitted with the Drude model to determine their charge carrier concentration, mobility and the alternating current (AC) resistivity. The highest values of mobility and charge carrier concentration were 8.31cm^2/Vs and 2.14 x 10^{21}cm^{-3} respectively. The lowest value of the AC resistivity was given by the ZnO:Al film with the highest value of the product (Nμ) of charge carrier concentration (N) and mobility (μ). The DC and AC resistivity were of the same orders of magnitude. The optical bandgap was found to increase with the increase in charge carrier concentration. A linear variation of $N^{2/3}$ with the optical bandgap, which concurs with the Burstein-Moss shift theory, was obtained.

Keywords: ZnO:Al, PEM, Drude model, transmittance, reflectance, sputtering.

INTRODUCTION

The use of aluminium doped zinc oxide (ZAO) as a transparent conductive oxide (TCO) has gained importance with the beginning of Cu(In,Ga)Se_2 (CIGS)-based thin-film module production (May *et al.* 2003). It has turned out to be the best suited TCO material with respect to its electro-optical properties, electronic and lattice matching to the absorber (Menner *et al.* 2011). ZnO-based TCO thin films are less expensive, non-toxic and have a simple production process (Lin *et al.* 2011). ZnO:Al films are commonly prepared by magnetron sputtering. Compared to other thin film deposition methods such as evaporation, chemical vapour deposition (CVD) or spray pyrolysis, magnetron sputtering is characterized by several advantages such as low substrate temperatures down to room temperature, good adhesion of films on substrates, high deposition rates, very good thickness uniformity, high density of the films, good controllability and long-term stability of the process (Dao *et al.* 2009).

The properties of ZnO:Al films depend on the deposition conditions (Zhu *et al.* 2010, Horwat *et al.* 2007, Igasaki *et al.* 2001). Oxygen partial pressure is one of the most critical parameters in determining the resistivity and the optical transmission of the ZnO:Al films. For TCO applications, there exists an optimum range of oxygen flow rate where the most favourable balance between the divergent requirements of low film resistivity and high optical transmission can be achieved (Brehme *et al.* 1999). Such films have been reported to be of columnar structures and consist of crystallites with significantly smaller sizes. In such case the comparison of electrical and infrared optical

measurements can help to give useful insight into the transport limiting processes. In contrast to standard DC methods, the measurement at optical frequencies present an alternative access to the study of carrier scattering processes monitoring the electronic transport at AC conditions during very short period of the carrier drift motion (Brehme *et al.* 1999). Thus, the electronic transport might be probed within dimensions which are smaller than the grain sizes. Drude model has been one of the favourites approach in studying the electronic transport at AC conditions as can be substantiated by several reports (Dao *et al.* 2009, Brehme *et al.* 1999, Sittinger *et al.* 2010).

Dao *et al.* (2009) reported on the electrical properties of reactive DC sputtered ZnO:Al derived from optical spectra using Drude model. They sputtered ZnO and Al_2O_3 targets in the argon and oxygen atmosphere and controlled the instability of the reactive process by using high pressure pumps. The report of their work focused on the changes of resistivity with the oxygen partial pressure. Sittinger and his co-workers (2010) derived electrical parameters from optical spectra after fitting the measured spectra with the Sernelius's and Drude models. They used the oxygen partial pressure variations to investigate the oxidation states of the target. They sputtered ZnO and Al targets in the oxygen atmosphere to prepare ZnO:Al films.

There are still few reports in the literature on the derivation of electrical properties of reactively sputtered ZnO:Al films from their optical spectra. The reports combining both the oxygen pressure deposition parameter and PEM control system for DC reactive ZnO:Al films are even fewer. To the best of our knowledge, no work has reported on optically derived electrical properties from sputtered Zn:Al metallic targets using Drude model.

In the current we discuss on the optical and electrical properties of ZnO:Al films prepared by sputtering Zn:Al metallic target in the oxygen atmosphere under controlled reactive process. The introduction of oxygen gas into the chamber and the control of instabilities during the reactive process were done by the plasma emission monitoring (PEM) system. The comparison of Drude's fittings for the metallic, compound/transition and insulating/reactive modes are discussed.

LITERATURE REVIEW

The Drude Model

The Drude parameters are involved in the classical oscillator model for free carriers where the real part of the dielectric function can be written (Brehme *et al.* 1999) as:

$$\varepsilon_1 = \varepsilon_\infty - \frac{\omega_\rho}{w^2 + \gamma^2} 2 \qquad (1)$$

Where, ε_∞, is the high-frequency dielectric constant including the interband contribution, γ, the damping constant and ω_p is the plasma frequency.

The damping constant, γ is related to the mobility, _ by the relation (Sing *et al.* 2001)

$$\gamma = \frac{e}{\mu m_e *} \qquad (2)$$

And the plasma frequency, ω_p is related to the charge carrier concentration, N by the relation (Brehme *et al.* 1999)

$$\omega_\rho{}^2 = \frac{Ne^2}{\varepsilon_0 \varepsilon_\infty m_e *} \qquad (3)$$

e is the electron charge, m_e* is the effective mass of electron in the conduction band and

ε_o is the permittivity of free space. $m_e^* = 0.28m_e$, where m_e is the free electron mass.
The AC resistivity, ρ_{AC} is determined from the relation (Jong *et al.* 2003)

$$\rho_{AC} = \frac{\gamma m^*}{Ne^2} = \frac{1}{\mu Ne} \quad (4)$$

Optical Bandgap Energy

The general formula for determining the optical bandgap (E_{opt}) is given by (Harding *et al.* 1991) as

$$(\alpha h\nu)^{1/n} = B(h_-E_{opt}) \quad (5)$$

Where B is a constant and *n* depends on the type of transition. For the indirect allowed, direct forbidden and direct allowed transition the values of *n* are 2, $\frac{3}{2}$ and $\frac{1}{2}$ respectively.

ZnO:Al involves a direct allowed transition and its corresponding relation (Harding *et al.* 1991) is

$$(\alpha h\nu)^2 = B(h\nu - E_{opt}) \quad (6)$$

The optical bandgaps are obtained by extrapolating the plot of $(\alpha h\nu)^2$ against $h\nu$, in which the x- intercept on the x- axis ($\alpha = 0$), gives E_{opt}, the optical bandgap.

The absorption coefficient of the films is calculated using the equation (Harding *et al.* 1991)

$$\acute{a} = \frac{1}{d}\ln\left[\frac{(1-R)^2}{2T} + \left\{\frac{(1-R)^4}{4T^2} - R^2\right\}^{0.5}\right] \quad (7),$$

where d stands for the film thickness, R is the reflectance and T is the transmittance.

2.3 The Burstein- Moss shift

The Burstein-Moss-Shift as an absorption edge effect because of conduction band filling with free carriers has usually been used for interpreting the experimental variation of bandgaps (Bender *et al.* 1998). Assuming parabolic band edges, the energy gap is given by

$$E_{opt} = E_{g,0} + \Delta E_g^{BM} \quad (8)$$

where

E_g^0 is the optical bandgap, (E_{opt}), $E_{gap,0}$ is the bandgap of the intrinsic material and ΔE_g^{BM} is the Burstein-Moss shift described as

$$\Delta E_g^{BM} = \frac{h^2}{2m^*_{vc}}\left(3\partial^2 N\right)^{\frac{2}{3}} \quad (9),$$

where m^*_{vc} is the combined reduced effective mass.

Therefore,

$$E_{opt} = E_{g,0} + \frac{h^2}{2m^*_{vc}}\left(3\partial^2 N\right)^{\frac{2}{3}} \quad (10).$$

Equation (10) suggests that E_{opt} varies linearly with $N^{2/3}$.

EXPERIMENTAL DETAILS

DC sputtered ZnO:Al films were deposited in stationary mode on a 5 x 5cm^2 glass substrates in a high vacuum system (VON ARDENNE ENLARGENTECHNIK GMBH). The chamber was evacuated to an ultimate pressure of 1 x 10^{-7}Torr, before introducing the argon gas (purity 99.9997%) through the mass flow controller. Then the metallic Zn:Al (Zn 98% + Al 2%) target with radius 5 cm was pre-sputtered for about ten minutes to remove any oxide layers resulting from air exposure. The oxygen gas (purity 99.998 %) was thereafter introduced into the chamber via a PEM control system which was controlling the amount of oxygen in the chamber. In the current work the 214nm zinc light emission line was used. The DC power was fixed at 200W.

The transmittance (T) and reflectance (R), measurements were carried out at room temperature using unpolarized light at normal incidence in the wavelength range 300 - 2500nm, with a double-beam spectrophotometer (Perkin Elmer Lambda

900) equipped with an integrating sphere coated with $BaS0_4$. The sheet resistance, which was used for the D.C resistivity determination was measured by using a Veeco FPP four-point probe. The film thickness measurements were done by using a Dektak 2000 Si surface profilometer after producing a step by etching. The films thickness were in the range 404-634nm.

The charge carrier concentration, mobility and AC resistivity of the films were determined from fitting into Drude model. The exercise involved four stages, namely: defining the optical constants in which the high frequency permeability, $\varepsilon_\infty = 3.85$ was used, since the literature (Jin *et al.* 1988), shows that $\varepsilon_\infty = 3.85 \pm 0.1$ irrespective of the doping; defining layer stacks; simulating spectra and fitting the parameters. The layer stack was vacuum/ZnO:Al/glass/vacuum and the simulated spectra were the transmittance(T) and reflectance (R). The fitting parameters employed were the damping constant (γ), plasma frequency (ω_p) and film thickness (t). The experimental data spectrum was fitted to the Drude's simulated spectrum by varying the mentioned fitting parameters. The fitting parameter values of the simulated spectrum were then used in the calculations of charge carrier concentration, mobility and AC resistivity.

RESULTS AND DISCUSSIONS

The fitting to the Drude model (optical properties)

Figures 1(a)-1(c) show the fittings to the Drude model of the simulated and measured spectra for the insulating, optimal, and metallic films deposited at 50%, 62% and 80% PEM setpoints respectively. There is a good Drude model fitting for all films with the exceptional of the metallic sample, which has a poor fitting. It had a very low transmittance, which made it difficult to do the transmittance fitting.

It is also worth noting that the transmittance increases with the decrease in PEM setpoints. This agrees well with the working principle of PEM, in which the PEM setpoint varies inversely with the oxygen pressure. At 100% PEM setpoints, there is Zn only (no oxygen) and at 0% PEM setpoint there is oxygen only (no Zinc). The insulating sample has higher transmittance in the infra-red region, which is possibly due to the decrease in free charge carriers.

In the case of reflectance, films deposited at higher PEM setpoints have higher reflectance on the entire 300-2500nm range, which is a typical Al particle absorption. The ZnO:Al film deposited at the PEM setpoint of 62% has the highest infrared reflectance. This is in agreement with the classical Drude theory, in which the IR reflectance, R increases with the increase in the product of charge carrier concentration (N) and mobility (_), N_ (Mosba, A., Aida, M.S 2012) i.e.

$$R = 1 - \frac{4\varepsilon_0 c_0}{e} \frac{1}{Nd\mu} \qquad (11)$$

where ε_0, c_0 and d represents the permittivity in free space, speed of light in vacuum and the film thickness respectively. Results from Table 1 indicate that the sample deposited at 62 % PEM setpoint (the highest reflecting TCO in the current work) has the highest value of $N\mu$.

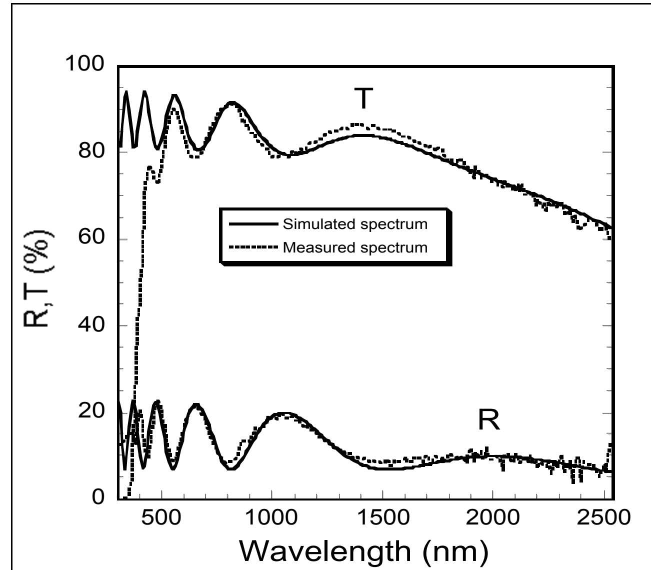

Figure 1(a): The simulated and measured spectrum for the insulating ZnO:Al film, deposited at 50 % PEM setpoint (power 200 W, sputtering pressure 3 mTorr, argon flow rate 10 sccm, deposition time 5 minutes).

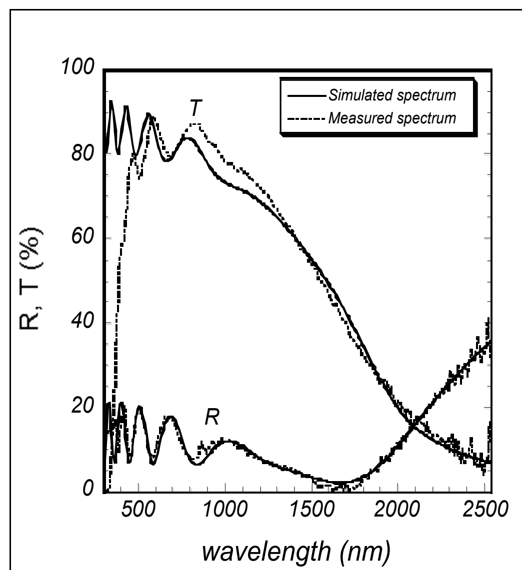

Figure 1(b) The simulated and measured spectrum for the metallic ZnO:Al film deposited at 62% PEM setpoint (power 200 W, sputtering pressure 3 mTorr, argon flow rate 10 sccm, deposition time 5 minutes).

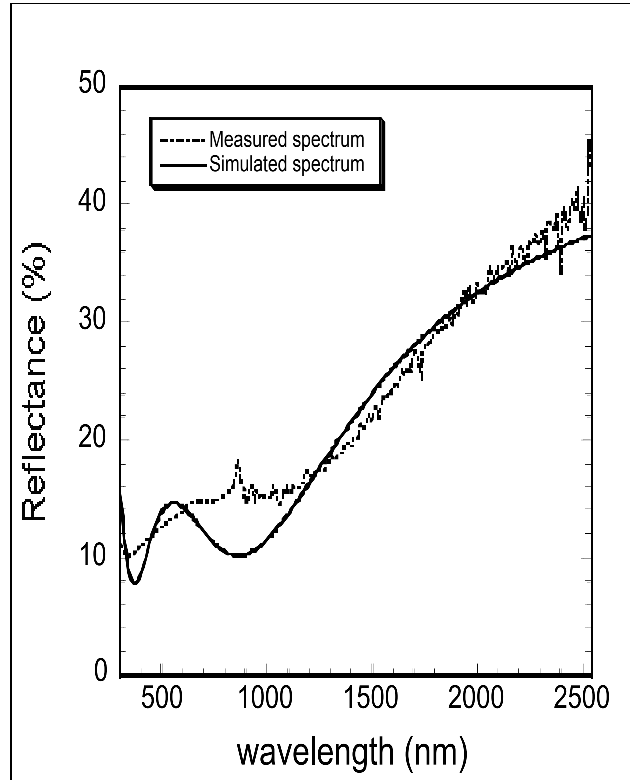

Figure 1(c): The simulated and measured spectrum for the composite film deposited at 80 % PEM setpoint (power 200 W, sputtering pressure 3 mTorr, argon flow rate 10 sccm, deposition time 5 minutes).

Optical bandgap

Figure 2 (a) illustrates the way, optical bandgaps were determined through extrapolation of the plot $(\alpha h\upsilon)^2$ against $h\upsilon$. The variation of optical bandgaps with PEM setpoints is shown by Figure 2 (b). The results show the increase in optical bandgaps with the increase in PEM setpoints. The increase in optical bandgap with the increase in PEM setpoints is mainly due to the Burstein-Moss effect, in which the optical bandgap widens due to the shift in Fermi level position in the conduction band brought by high charge carrier density of ZnO:Al films (Szyska *et al.* 2003). Optical bandgaps for metallic films, deposited at PEM setpoints 70 and 80 % could not be obtained due to the extremely low transmittance.

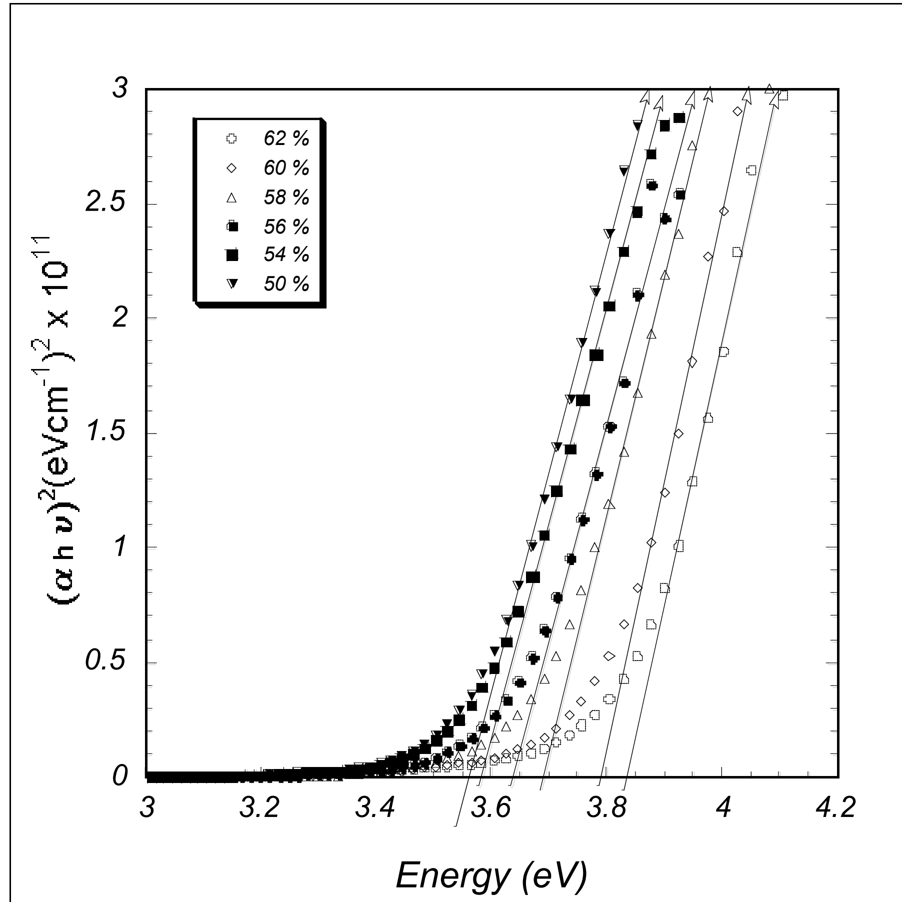

Figure 2 (a): The plot of $(\alpha h\upsilon)^2$ with energy $h\upsilon$ for the determination of optical bandgaps of ZnO:Al films.

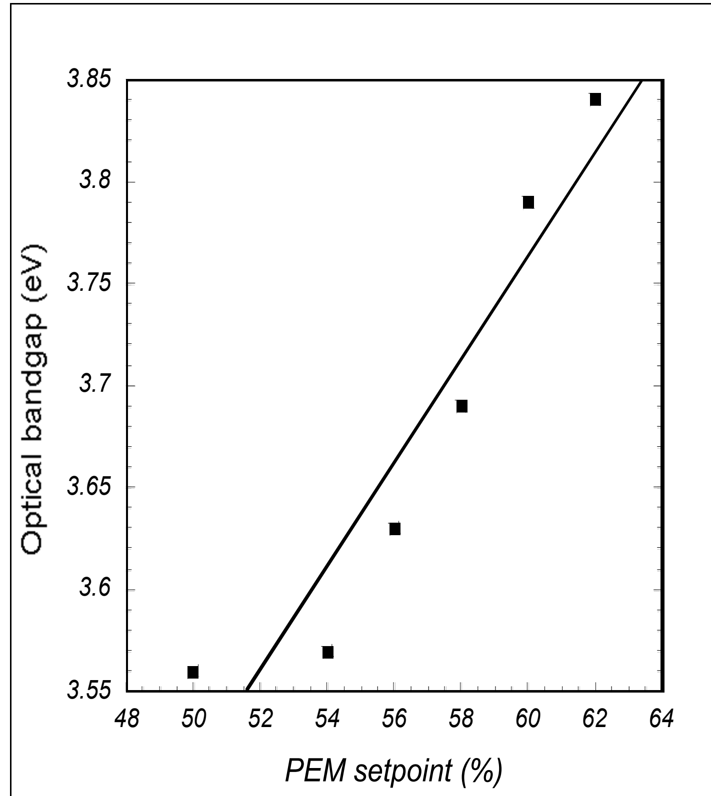

Figure 2 (b): The variation of optical bandgap with PEM setpoints (DC power 200 W, argon flow rate 10 sccm, sputtering pressure 3 mTorr, deposition time 5 minutes).

The Burstein-Moss Shift is always studied by plotting $N^{2/3}$ against the optical bandgap of the given material as shown by Figure 3.

There is a linear relationship of the two mentioned quantities verifying that the increase in optical bandgap with charge carrier concentration is due to the Burstein-Moss Shift.

Electrical properties

Charge carrier concentration and mobility

The changes in charge carrier concentrations and mobility with PEM setpoint is shown in Figure 4. The charge carrier concentration increases and the mobility decreases with the increase in PEM setpoints. At higher PEM setpoints there is low oxygen content in the ZnO:Al films, while at lower PEM setpoints it is the opposite. The decrease in charge carrier concentration with PEM setpoint is due to the suppression of oxygen vacancies by oxygen atoms (Martinez *et al.* 1997). The increase in mobility is possibly due to the improvement in crystallinity of the films (Wang *et al.* 2005).

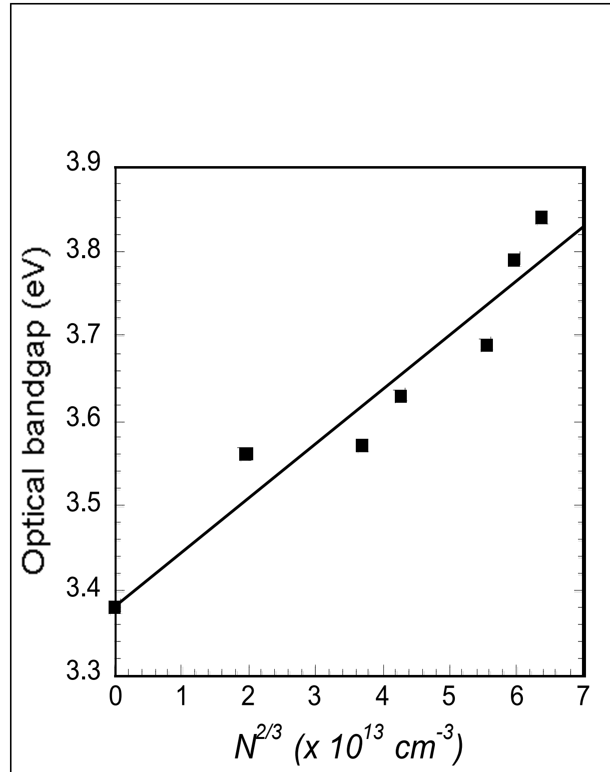

Figure 3: Optical bandgap (E_{opt}) against $N^{\frac{2}{3}}$ for reactive DC sputtered ZnO:Al films prepared under different PEM setpoints (DC power 200 W, argon flow rate 10 sccm, sputtering pressure 3 mTorr, deposition time 5 minutes).

This result is similar to the results from other works (Martinez *et al.* 1997, Brehme *et al.* 1999) who reported on the decrease of charge carriers with increase in oxygen flow rate. Agashe and his co-workers (2003) reported on similar results as they found a drop in mobility from $44cm^2/Vs$ to $23cm^2/Vs$ with an increase in carrier concentration from $2 \times 10^{20}cm^3$ to $9 \times 10^{20}cm^3$ for RF sputtered ZnO:Al films. The data for the PEM setpoints, charge carrier concentration, mobility and the product of mobility and charge carrier concentration is summarized by Table 1.

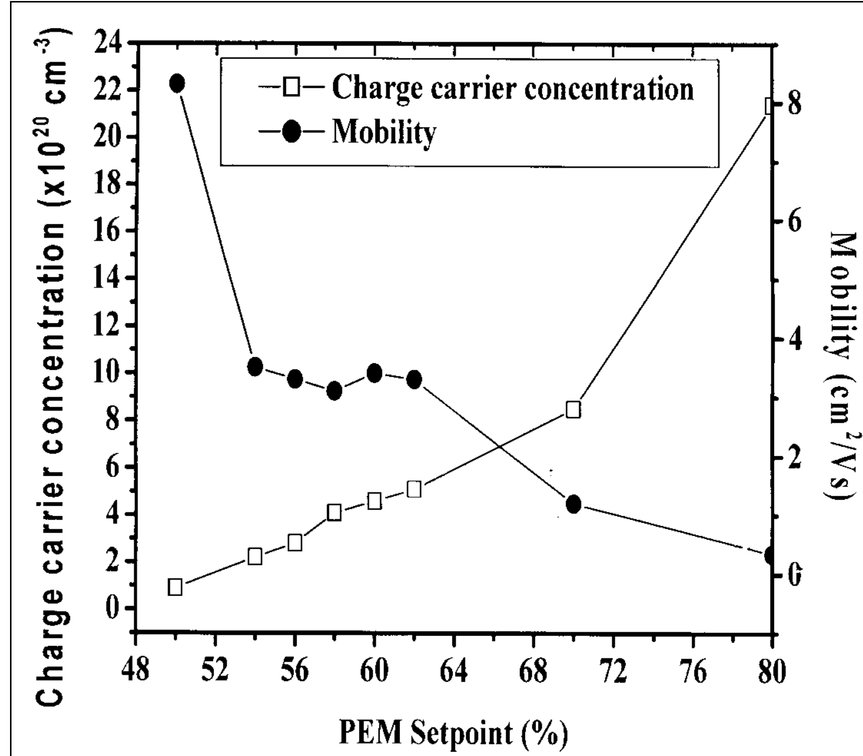

Figure 4 Changes of charge carrier concentration and mobility with PEM setpoints (DC power 200 W, argon flow rate 10 sccm, sputtering pressure 3 mTorr, deposition time 5 minutes).

Table 1: Values of charge carrier concentration (N), mobility (μ) and the product Nμ for ZnO:Al prepared at various PEM setpoints.

PEM setpoint (%)	N (cm^{-3})	μ (cm^2/Vs)	Nμ (cm^{-1}/Vs)
50	8.89×10^{19}	8.31	7.4×10^{20}
54	2.24×10^{20}	3.53	7.9×10^{20}
56	2.78×10^{20}	3.3	9.2×10^{20}
58	4.12×10^{20}	3.1	12.8×10^{20}
60	4.62×10^{20}	3.42	15.8×10^{20}
62	5.08×10^{20}	3.3	16.8×10^{20}
70	8.45×10^{20}	1.22	10.4×10^{20}
80	2.14×10^{21}	0.34	7.1×10^{20}

Resistivity

The changes of AC and DC resistivity with PEM setpoints is shown in Figure 5. The trend for both AC and DC resistivity is similar. The resistivity decreases with the PEM setpoint up to 62% PEM setpoint before increasing for PEM setpoints greater than 62%. At lower PEM setpoints the target oxidation leads to formation of Al_2O_3 phase, which decreases the carrier concentration and increase the mobility which eventually leads to the increase of the resistivity (Jong *et al.* 2003). The slight increase in resistivity with PEM setpoints beyond 60% PEM setpoint is possibly due to the formation of an Al-ZnO composite giving a lower charge carrier concentration in the ZnO (Hu J & Gordon R 1991).

The results indicate that the values of AC resistivity from Drude model are relatively higher than those of DC resistivity from the four point probe. The DC is measured under DC conditions and should involve all scattering processes which control the lateral electron transport in the film including the scattering at the grain boundaries. The AC resistivity on the other hand is obtained by sampling the carrier motion at optical frequencies where the monitored transport paths are smaller than the grain size and thus the probability of crossing a grain boundary is low (Brehme *et al.* 1999). So, the opposite was expected. Similar results were reported elsewhere (Brehme *et al.* 1999), whereby they found out that the AC conductivity of ZnO:Al films was lower than the DC counterpart. Apparently, there are no clear reasons for such discrepancy, which calls for further investigations. There is a coincidence of the AC and DC resistivity at 50% PEM setpoint suggesting that at higher oxygen pressures, both quantities are limited by the same scattering process taking place within the volume of the grains. Brehme *et al.* (Brehme *et al.* 1999) reported on a similar coincidence at higher oxygen flow rates. The minimum resistivity is found to be on the 60-62% PEM setpoints range.

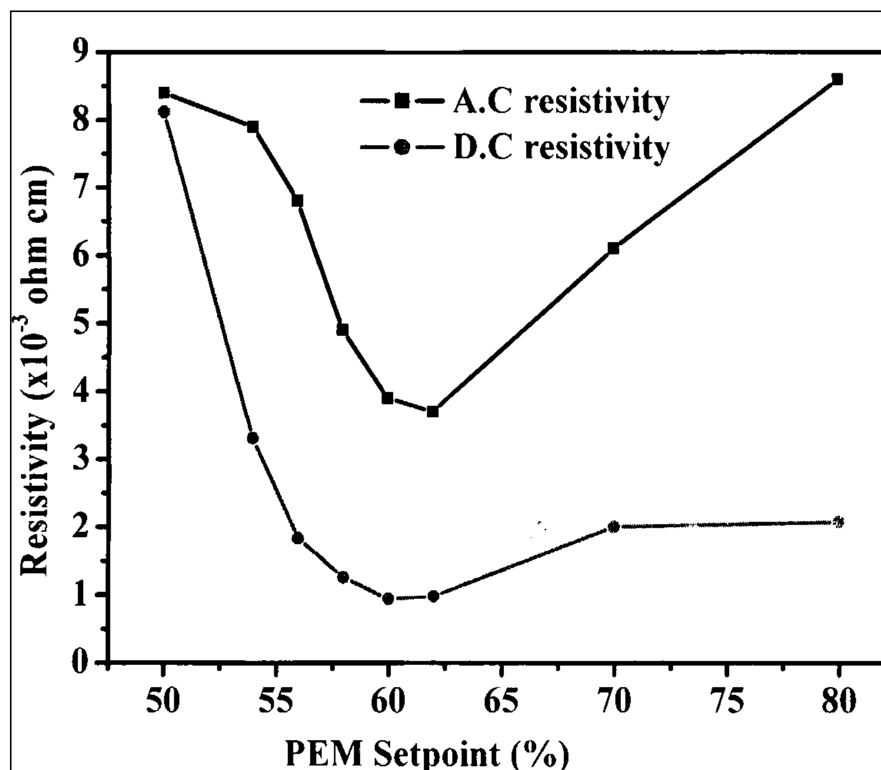

Figure 5: The variation of A.C and D.C resistivity with the PEM setpoint. (DC power 200 W, argon flow rate 10 sccm, sputtering pressure 3 mTorr, deposition time 5 minutes)

CONCLUSION

DC reactive sputtered ZnO:Al films with low resistivity and high transmittance have successfully being produced using a plasma emission monitoring (PEM) control system. The Drude model seems to fit quite well with ZnO:Al films with the exception of the film deposited at 80 % whose transmittance was too low. The AC data from Drude model were comparable to experimental D.C data. The charge carrier concentration increased and the mobility decreased with the increase in PEM setpoints. Low resistive ZnO:Al films were produced in the range 60-62% PEM setpoints. The optimal film, deposited at 62% PEM setpoint had the highest _N product. The optical bandgaps increased from 3.56 to 3.84eV with the increase in PEM setpoints from 50 to 62%. This relationship is confirmed from equation (10).

ACKNOWLEDGEMENTS

One of the authors, Nsimama, P.D wishes to express his appreciation to the IPPS, Uppsala-Sweden, for their financial support to the current work. Prof. Gunnar Niklasson is highly acknowledged for his constructive inputs in the results and discussion. The moral encouragement and support from Prof. Lennart Hasselgren is profoundly appreciated.

REFERENCES

Agashe C, Kluth O, Schöpe G, Siekmann H, Hupskes J and Rech B 2003 Optimization of the electrical properties of magnetron sputtered aluminum-doped

zinc oxide films for opto-electronic application. *Thin Solid Films* **442**:157-172.

Bender M, Seelig W, Daube C, Frankenberger H, Ocker B and Stollenwerk J 1998 Dependence of oxygen flow on optical and electrical properties of DC-magnetron sputtered ITO films. *Thin Solid Films* **326**:72-77.

Brehme S, Fenske F, Fuhs W, Nebauer E, Poschenrieder M, Selle B and Sieber I, 1999 Free-carrier plasma resonance effects and electron transport in reactively sputtered degenerate ZnO:Al films. *Thin Solid Films* **342**:167-173.

Dao VA, Le T, Tran T, Nguyen H, Kim K, Lee J, Jung S, Lakshminarayan N and Yi J 2009 Electrical and optical studies of transparent conducting ZnO:Al thin films by magnetron dc sputtering. *J. Electroceram*. **23**:356-360**.**

Harding GL, Window B and Horrigan EC 1991 Aluminium-and indium doped zinc oxide thin films prepared by DC magnetron reactive sputtering. *Sol. Energy Mater. Sol. Cells* **22**:69-91.

Hong RJ, Jiang X, Szyszak B, Sittinger V and Pflug A 2003 Studies on ZnO:Al thin films deposited by in-line reactive mid-frequency magnetron sputtering. *Appl. Surf. Sci.* **207**:341-350.

Horwat D and Billard A 2007 Effects of substrate position and oxygen gas flow rate on the properties of ZnO:Al films prepared by reactive co-sputtering. *Thin Solid Films* **515**:5444-5448.

Igasaki Y and Kanma H 2001 Argon gas pressure dependence of the properties of transparent conduction ZnO:Al films deposited on glass substrates. *Appl. Surf. Sci.* **169–170**:508-511.

Jin ZC, Hamberg, I and Granqvist CG 1988 Optical properties of sputter-deposited ZnO:Al thin films. *J. Appl. Phys.* **64**:5117-5131.

Lin YC, Wang BL, Yen WT and Shen CH 2011 Surface textured molybdenum doped zinc oxide thin films prepared for thin film solar cells using pulsed direct current magnetron sputtering. *Thin Solid Films* **519**:5571-5576.

Martinez MA, Herrero J and Gutierrez MT 1997 Deposition of transparent and conductive Al-doped ZnO thin films for photovoltaic solar cells. *Sol. Energy Mater. Sol. Cells* **45**: 75-86.

May C, Menner R, Strumpfel J, Oertel M and Sprecher B 2003 Deposition of TCO films by reactive magnetron sputtering from metallic Zn:Al alloy targets. *Surf. Coat. Technol*. **169-170**: 512-516.

Menner R, Hariskos D, Linss V and Powalla M 2011 Low-cost ZnO:Al transparent contact by reactive rotatable magnetron sputtering for Cu(In,Ga)Se_2 solar moddules. *Thin Solid Films* **519**:7541-7544.

Mosbah A and Aida MS 2012 Influence of deposition temperature on structural, optical and electrical properties of sputtered Al doped ZnO thin films. *J. Alloy Compd*. **515**:149-153.

Singh AV, Kumar M, Mehar RM, Wakahar A and Yoshida A 2001 Al-doped zinc (ZnO:Al) thin films by pulsed laser ablation. *J. India Inst. Sci.* **81**: 527.

Sittinger V, Ruske F, Pflug A, Dewald W, Szyszka B and Dittmar G 2010 Optical on-line monitoring for the long-term stabilization of a reactive mid-frequency sputtering process of Al-doped zinc oxide films. *Thin Solid Films* **518**:3115-3118.

Szyszka B, Sittinger V, Jiang X, Hong RJ, Werner W, Pflug A, Ruskeb M and Lopp A 2003 Transparent and conductive ZnO:Al films deposited by large area reactive magnetron sputtering. *Thin Solid Films* **442**:179-183.

Wang W.W, Diao X.G, Wang Z, Yang M, Wang T.M and Wu Z 2005 Preparation and characterization of high-performance direct current magnetron sputtered ZnO:Al films. *Thin Solid Films* **491**:54 – 60.

Zhu H, Hüpkes J, Bunte E and Huang SM 2010 Oxygen influence on sputtered high rate ZnO:Al films from dual rotatable ceramic targets. *Appl. Surf. Sci.* **256**:4601-4605.